JETIR.ORG ISSN: 2349-5162 | ESTD Year : 2014 | Monthly Issue
JOURNAL OF EMERGING TECHNOLOGIES AND INNOVATIVE RESEARCH (JETIR)
An International Scholarly Open Access, Peer-reviewed, Refereed Journal

Review and Comparison of Non-Isolated DC-DC Converters for Electric Vehicle Applications

[1]Smitha Joseph

[1]Lecturer in Electrical and Electronics Engineering,
[1]Department of Electrical and Electronics Engineering,
[1]Government Polytechnic College, Kalamassery, Kerala, India.

Abstract : The fast growth of the electric vehicle market has intensified research on power electronic converters that enable efficient energy management within vehicle powertrains. Among these, non-isolated DC-DC converters have emerged as attractive solutions for applications where galvanic isolation is not mandatory, offering advantages in terms of reduced size, weight, and improved efficiency compared to their isolated counterparts. This paper presents a comprehensive review and comparison of non-isolated DC-DC converter topologies for EV applications, covering literature published through 2023. The review encompasses fundamental topologies including Buck, Boost, and Buck-Boost variants, as well as advanced configurations such as interleaved, bidirectional, high step-up, multi-input, and partial power processing converters. A systematic taxonomy is developed to classify these topologies based on voltage conversion function, power flow direction, and gain enhancement techniques. Quantitative comparisons are provided for key performance metrics including efficiency ranging from 88% to 99%, voltage gain capability, component count, and switch voltage stress. The paper also examines emerging technologies such as wide bandgap semiconductors and their impact on converter performance. Research gaps are identified, and future research directions are proposed. Finally, application-specific recommendations are provided to guide topology selection for various EV subsystems including auxiliary power supply, fuel cell integration, on-board charging, and vehicle-to-grid applications.

***IndexTerms* - Non-isolated DC-DC converter, electric vehicle, power electronics, high step-up converter, bidirectional converter, partial power processing, wide bandgap semiconductors.**

I. INTRODUCTION

The worldwide shift towards sustainable transportation has accelerated the adoption of electric vehicles at an unprecedented rate. According to the International Energy Agency, global EV sales exceeded 10 million units in 2022, representing a 55% increase from the previous year, with projections indicating continued exponential growth through the decade [1]. This rapid electrification of the transportation sector has created substantial demand for efficient, compact, and cost-effective power electronic systems that form the backbone of EV powertrains. DC-DC converters constitute critical components within EV power architectures, serving multiple essential functions. These include interfacing the high-voltage traction battery with the propulsion system, providing power to low-voltage auxiliary loads such as 12V or 48V systems, enabling on-board and off-board battery charging, and facilitating vehicle-to-grid power transfer capabilities [2]. The performance characteristics of these converters, particularly efficiency, power density, and reliability, directly impact vehicle range, charging time, and overall system cost.

DC-DC converters are broadly classified into isolated and non-isolated topologies based on the presence of galvanic separation between input and output sides. Isolated converters employ high-frequency transformers to provide electrical isolation, which is essential in applications requiring safety isolation, ground loop elimination, or large voltage conversion ratios. However, the transformer introduces additional losses, increases size and weight, and adds manufacturing complexity [3]. Non-isolated converters, in contrast, eliminate the transformer, resulting in several key advantages for EV applications. First, the absence of magnetic isolation components reduces converter volume by 30-50% and weight proportionally, which is critical for vehicle efficiency and packaging [4]. Second, elimination of transformer core and winding losses enables efficiency improvements of 2-5% compared to equivalent isolated topologies [5]. Third, simplified construction with fewer components reduces manufacturing costs by approximately 20-30% [6]. Fourth, reduced component count facilitates easier thermal management and improves reliability. Non-isolated topologies are particularly suitable for EV applications where the input and output share a common ground reference and safety isolation is achieved through other means, such as the battery management system or vehicle isolation monitoring [7].

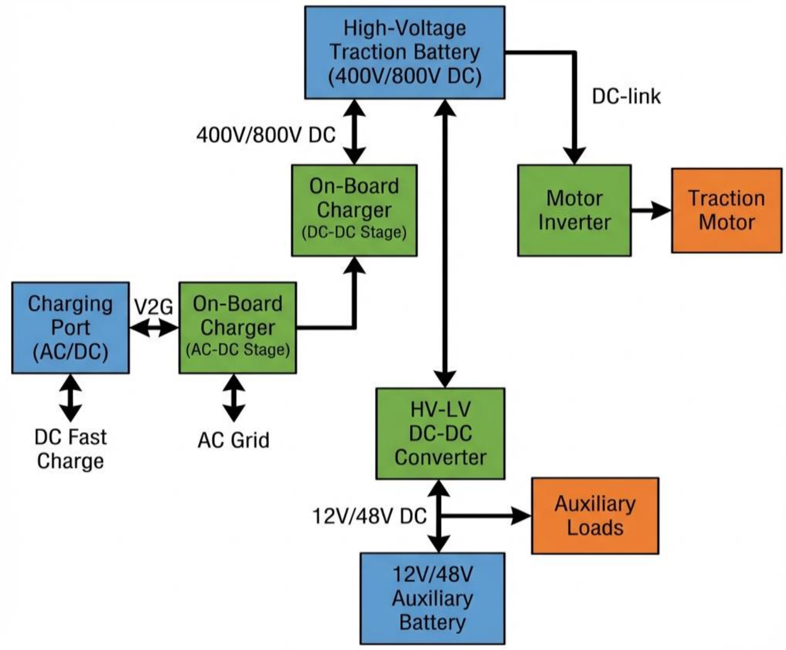

Figure 1: EV Power Architecture with DC-DC Converter Locations

The above figure illustrates the typical power architecture of an electric vehicle, highlighting the locations where DC-DC converters interface various system components. The high-voltage traction battery connects to the motor inverter through the DC-link, while HV-LV DC-DC converters supply the 12V and 48V auxiliary systems. The on-board charger incorporates both AC-DC and DC-DC conversion stages, with bidirectional capability enabling V2G power transfer.

This paper provides a comprehensive review and comparison of non-isolated DC-DC converter topologies specifically designed for or applicable to electric vehicle systems. The key contributions include a comprehensive taxonomy of non-isolated DC-DC converter topologies organized by voltage conversion function, power flow direction, number of ports, and gain enhancement technique. The paper provides detailed analysis of six major topology categories comprising basic converters, interleaved converters, high step-up converters, bidirectional converters, multi-input converters, and partial power processing converters. Quantitative comparison of topologies based on efficiency, voltage gain, component count, switch stress, and application suitability is presented. The review examines emerging technologies including wide bandgap semiconductors and their impact on converter performance. Research gaps and future research directions in the field are identified. Application-specific recommendations for topology selection across various EV subsystems are provided.

The remainder of this paper is organized as follows. Section II presents the classification and taxonomy of non-isolated DC-DC converters for EV applications. Section III provides detailed analysis of individual topology categories. Section IV presents comparative analysis across topologies using multiple performance metrics. Section V discusses emerging technologies and trends. Section VI identifies research gaps and proposes future directions. Section VII concludes the paper with summary remarks and recommendations.

II. Classification and Taxonomy

2.1 Classification Criteria

Non-isolated DC-DC converters for EV applications can be classified according to multiple criteria, each highlighting different aspects of converter functionality and design characteristics. Firstly, classification by voltage conversion function distinguishes between step-down or Buck-derived converters, step-up or Boost-derived converters, and step-up/down or Buck-Boost-derived converters. Step-down converters are employed for high-voltage to low-voltage conversion, such as supplying 12V auxiliaries from a 400V battery. Step-up converters boost lower voltage sources, such as fuel cells, to the DC-link voltage. Step-up/down converters accommodate varying input-output voltage relationships, useful for wide battery state-of-charge ranges. Secondly, classification by power flow direction separates unidirectional converters, which transfer power in a single direction and are suitable for auxiliary power supplies, from bidirectional converters, which enable power flow in both directions and are essential for regenerative braking energy recovery and V2G applications.

Further, classification by number of inputs and outputs distinguishes single-input single-output converters representing the conventional configuration from multi-input single-output converters that integrate multiple energy sources such as combining battery, photovoltaic, and fuel cell inputs, and from multi-port converters that extend this concept to include multiple outputs for diverse load requirements. Finally, classification by gain enhancement technique identifies the various methods used to achieve high voltage conversion ratios including coupled inductors, switched capacitors, voltage multiplier cells, and cascaded structures.

2.2 Taxonomy of Non-Isolated DC-DC Converters

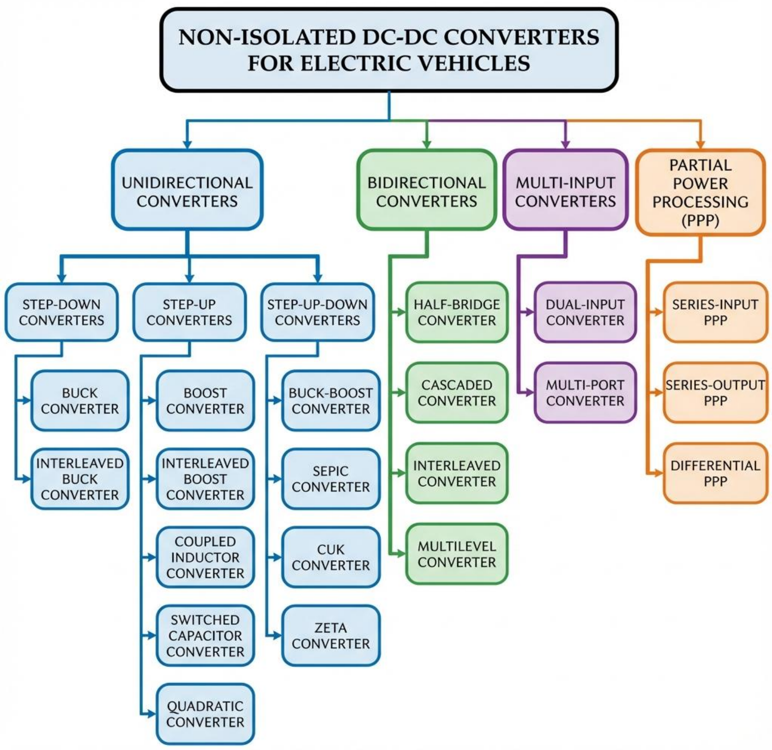

Figure 2: Taxonomy of Non-Isolated DC-DC Converters for Evs.

Figure 2 above presents a comprehensive taxonomy of non-isolated DC-DC converter topologies applicable to electric vehicle systems. The hierarchical structure organizes converters first by power flow direction, then by voltage conversion function, and finally by specific topology or gain enhancement technique.

The taxonomy encompasses four main branches. Unidirectional converters include step-down topologies such as Buck, interleaved Buck, and synchronous Buck configurations. Step-up topologies within this branch include Boost, interleaved Boost, coupled inductor Boost, switched capacitor Boost, and quadratic Boost converters. Step-up/down topologies comprise Buck-Boost, SEPIC, Cuk, Zeta, and Luo converters. Bidirectional converters encompass half-bridge configurations, cascaded Buck-Boost structures, interleaved bidirectional topologies, and multilevel bidirectional converters. Multi-input and multi-port converters include dual-input single-output configurations, multi-input Boost variants, and general multi-port architectures for hybrid energy source integration. Partial power processing converters represent an emerging category with series-input, series-output, and differential configurations designed for ultra-high efficiency in narrow voltage conversion applications.

2.3 Application Mapping

Table I maps converter topology categories to specific EV applications based on power requirements and functional needs. The selection criteria consider power level, voltage conversion ratio, bidirectional capability, efficiency requirements, and cost constraints.

Table I: Topology Selection by EV Application

Application	Power Range	Key Requirements	Recommended Topologies
HV-LV Auxiliary	1-3 kW	High step-down ratio, high efficiency	Synchronous Buck, Interleaved Buck
Fuel Cell Interface	5-30 kW	High step-up ratio, continuous input current	CI-Boost, Interleaved Boost
On-board Charging	3-22 kW	Power factor correction, bidirectional	SEPIC, Bridgeless Cuk
Off-board Fast Charging	50-350 kW	High power, modularity, efficiency	Interleaved, Modular configurations
Battery Balancing	10-100 W	Ultra-high efficiency, low cost	Partial Power Processing
V2G/V2H	5-15 kW	Bidirectional, wide voltage range	Cascaded bidirectional, Half-bridge

III. TOPOLOGY ANALYSIS

3.1 Basic Topologies

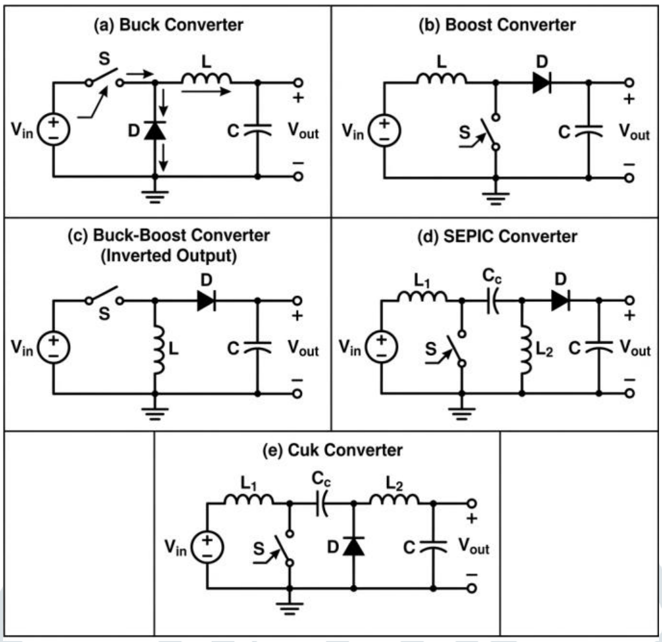

Figure 3: Five basic topology circuits (Buck, Boost, Buck-Boost, SEPIC, Cuk)

The Buck converter represents the fundamental step-down topology, producing an output voltage lower than the input according to the relationship where output voltage equals duty cycle multiplied by input voltage. In EV applications, Buck converters interface the high-voltage traction battery, typically 400V or 800V, with low-voltage auxiliary systems operating at 12V or 48V [8]. The conventional Buck converter uses a single switch, single diode, single inductor, and output capacitor. Synchronous Buck variants replace the diode with a second switch to reduce conduction losses, achieving efficiency improvements of 2-3% at typical operating points [9]. The topology offers inherent simplicity and high efficiency of 94-97% for moderate step-down ratios. Key limitations include discontinuous input current, which may require additional filtering at the input side, and limited practical duty cycle range. For very high step-down ratios such as 400V to 12V, the required duty cycle of approximately 3% creates challenges for control resolution and switching loss management.

The Boost converter provides step-up voltage conversion with an ideal voltage gain equal to input voltage divided by one minus the duty cycle. This topology finds application in fuel cell electric vehicles where the fuel cell stack voltage, typically 30-60V, must be boosted to match the DC-link voltage of 400V or higher [10]. The basic Boost topology consists of a single switch, diode, inductor, and output capacitor. While simple, the converter faces practical limitations at high voltage gains. As the duty cycle approaches unity to achieve high gains, conduction losses increase substantially, and switch voltage stress equals the output voltage. These constraints limit practical efficiency to 93-96% and maximum achievable gain to approximately 5-6× without auxiliary techniques [11]. The Buck-Boost converter family provides bidirectional voltage conversion capability, producing output voltage that can be higher or lower than the input. The basic inverting Buck-Boost converter achieves voltage gain with the output inverted relative to input polarity. The SEPIC topology eliminates output polarity inversion while maintaining step-up/down capability. It employs two inductors, which may be coupled, and a coupling capacitor, providing non-inverted output and continuous input current [12]. These characteristics make SEPIC attractive for battery charging applications where input current quality affects battery life. Reported efficiency ranges from 88-93% depending on operating point and design optimization.

The Cuk topology, like SEPIC, provides step-up/down capability with continuous input and output currents, a unique characteristic among basic converters [13]. The continuous output current reduces ripple stress on battery loads during charging. However, the inverted output polarity limits direct application. Bridgeless Cuk variants for power factor correction in EV chargers achieve 92-94% efficiency while providing unity power factor operation [14]. The Zeta converter offers non-inverted output with step-up/down capability but exhibits discontinuous input current, limiting its suitability for sensitive source applications such as fuel cells.

Figure 3 presents circuit schematics for the five basic non-isolated DC-DC converter topologies. Part (a) shows the Buck converter with its characteristic inductor in the output path. Part (b) illustrates the Boost converter with the inductor at the input. Part (c) depicts the inverting Buck-Boost configuration. Parts (d) and (e) show the SEPIC and Cuk converters respectively, highlighting their dual-inductor structures with coupling capacitors.

3.2 Interleaved Topologies

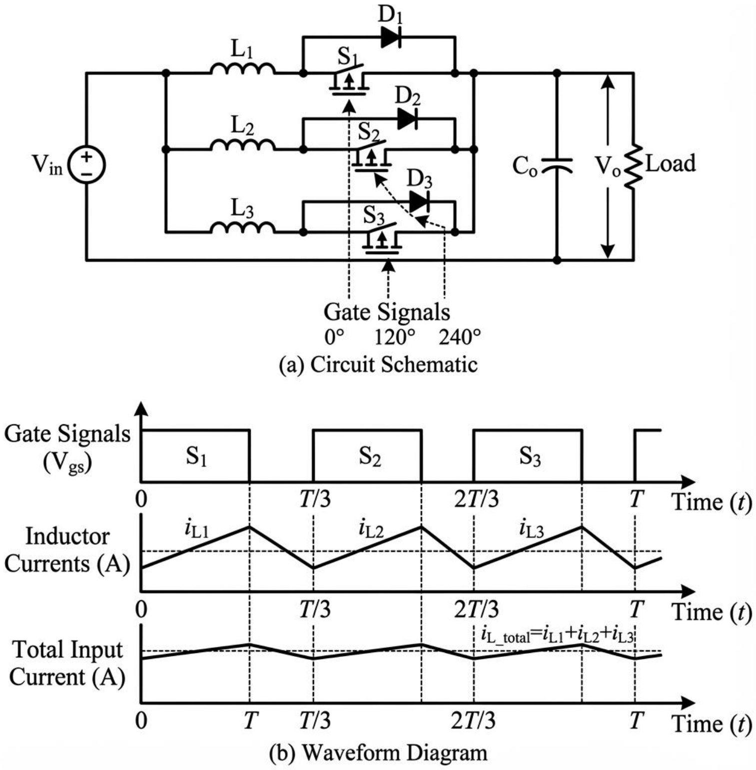

Figure 4: Three-phase interleaved boost converter and waveforms

Interleaving represents a fundamental technique for improving converter performance by operating multiple converter phases in parallel with phase-shifted switching signals. This approach offers several advantages critical for high-power EV applications [15].

In an N-phase interleaved converter, each phase operates with a switching signal phase-shifted by 360 degrees divided by N relative to adjacent phases. This phase shifting produces several beneficial effects. The input and output current ripples from individual phases partially cancel, with theoretical complete cancellation possible at certain duty cycles. For an N-phase interleaved Boost converter, input current ripple reduces by a factor proportional to N compared to a single-phase design operating at the same total power [16]. Additionally, power dissipation distributes across N phases rather than concentrating in a single power stage, reducing thermal stress on individual components and enabling smaller heatsinks or higher power density. Furthermore, the multi-phase structure provides inherent redundancy, allowing operation to continue at reduced power if individual phases fail.

Figure 4 illustrates a three-phase interleaved Boost converter topology and its characteristic waveforms. Part (a) shows the circuit schematic with three parallel Boost phases sharing common input and output connections, with each phase comprising an inductor, switch, and diode. Part (b) presents the switching waveforms demonstrating the 120-degree phase shift between gate signals and the resulting ripple cancellation in the total input current.

The interleaved Boost converter has received extensive attention for EV applications, particularly for fuel cell and photovoltaic integration. A three-phase interleaved step-up converter demonstrated 94% efficiency at 1 kW with 65% reduction in input current ripple and 33% reduction in switch voltage stress compared to single-phase operation [17]. Multi-phase interleaved Boost converters scale effectively to high power levels. Commercial implementations for FCEV applications operate at power levels exceeding 30 kW with efficiency above 96% [18]. The interleaved structure also facilitates digital control implementation with phase current balancing algorithms ensuring equal power sharing among phases.

For high-voltage to low-voltage conversion from HV to 12V or 48V, interleaved Buck converters address the high current requirements of auxiliary loads while minimizing output voltage ripple. A 4-phase interleaved synchronous Buck converter for 400V to 48V conversion achieved 97% efficiency at 2 kW output [19].

Table II: Interleaving Benefits Summary

Parameter	Single-Phase	2-Phase	3-Phase	4-Phase
Ripple Reduction	Baseline	50%	67%	75%
Phase Current	100%	50%	33%	25%
Component Count	Low	Medium	High	Higher
Control Complexity	Low	Medium	Medium	High
Reliability	Baseline	Improved	Higher	Highest

3.3 High Step-Up Topologies

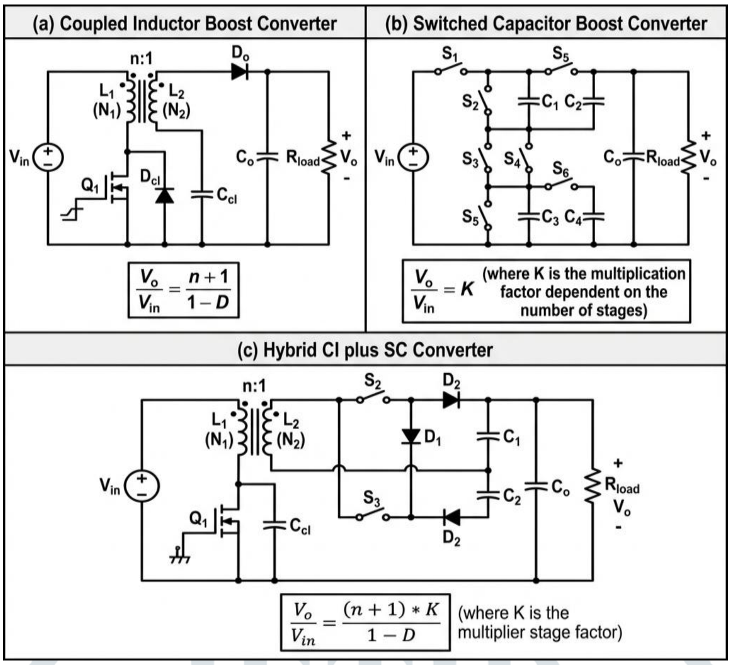

Figure 5: High Step-Up Converter Topologies (CI, SC, Hybrid)

Applications requiring voltage conversion ratios exceeding 5-6× necessitate advanced topologies that overcome the limitations of basic Boost converters. Several techniques enable high voltage gain while maintaining reasonable efficiency and manageable switch stress [20].

Coupled inductor topologies exploit transformer action to achieve voltage multiplication while maintaining non-isolated operation. The coupled inductor consists of primary and secondary windings on a shared magnetic core with turns ratio n. The voltage gain of a basic coupled-inductor Boost converter follows the relationship where gain equals n plus one, divided by one minus the duty cycle. For a turns ratio of 3 and duty cycle of 0.5, the voltage gain is 8×, substantially higher than the 2× achievable with a conventional Boost at the same duty cycle [21]. Critical advantages of coupled-inductor-based converters include reduced switch voltage stress, with the switch voltage clamped to a fraction of the output voltage, typically 0.3-0.4 times the output voltage, enabling use of lower-voltage rated devices with better performance characteristics. High voltage gains of 10-15× are readily achievable without extreme duty cycles. Properly designed clamping circuits capture and recycle leakage inductance energy, preventing voltage spikes and improving efficiency. Reported efficiency for coupled-inductor Boost converters ranges from 92-96% at power levels from 200W to several kilowatts [22].

Switched capacitor converters achieve voltage multiplication through periodic charging and discharging of capacitors in different configurations. Pure switched capacitor converters use only switches and capacitors without inductors, offering potential advantages in power density and magnetic-free operation [23]. The fundamental switched capacitor voltage doubler alternately charges a capacitor in parallel with the input and discharges it in series, producing 2× voltage gain. Cascading multiple stages or using more complex switching patterns achieves higher gains. However, efficiency drops significantly when operating away from the designed conversion ratio due to charge redistribution losses. Resonant switched capacitor converters address efficiency limitations by adding small inductors that enable soft charging, achieving nearly lossless charge transfer. Hybrid approaches combining switched capacitor voltage multiplication with inductive energy storage achieve both high gain and high efficiency of 93-97% across wider operating ranges [24].

Recent research has focused on combining coupled inductors and switched capacitors to synergistically achieve very high voltage gains with minimal switch stress. A converter employing both techniques demonstrated voltage gain of 13× at 50% duty cycle with switch voltage stress of only 20% of the output voltage [25]. The 400W prototype achieved 95.6% peak efficiency while boosting 30V input to 400V output, a conversion ratio highly relevant for fuel cell EV applications.

Figure 5 presents circuit schematics for three high step-up converter topologies. Part (a) shows the coupled inductor Boost converter with primary and secondary windings, clamp circuit, and output diodes. Part (b) illustrates a switched capacitor Boost converter with multiple switches and capacitors arranged for voltage multiplication. Part (c) depicts the hybrid topology combining coupled inductor and switched capacitor techniques to achieve ultra-high voltage gain with minimal switch stress.

Table III: High Step-Up Converter Comparison

Topology	Gain (D=0.5)	Switch Stress	Switches	Inductors	Efficiency
Basic Boost	2×	V_out	1	1	93-96%
CI-Boost	6-8×	0.3-0.4×V_out	1	1 (coupled)	92-96%
SC-Boost	4-6×	0.5×V_out	2-4	0-1	93-97%
Quadratic	4×	V_out	2	2	88-93%
CI+SC Hybrid	13×	0.2×V_out	1	1 (coupled)	94-96%

Table III compares high step-up converter topologies across key performance metrics, highlighting the trade-offs between voltage gain capability, switch stress, component count, and efficiency.

3.4 Bidirectional Topologies

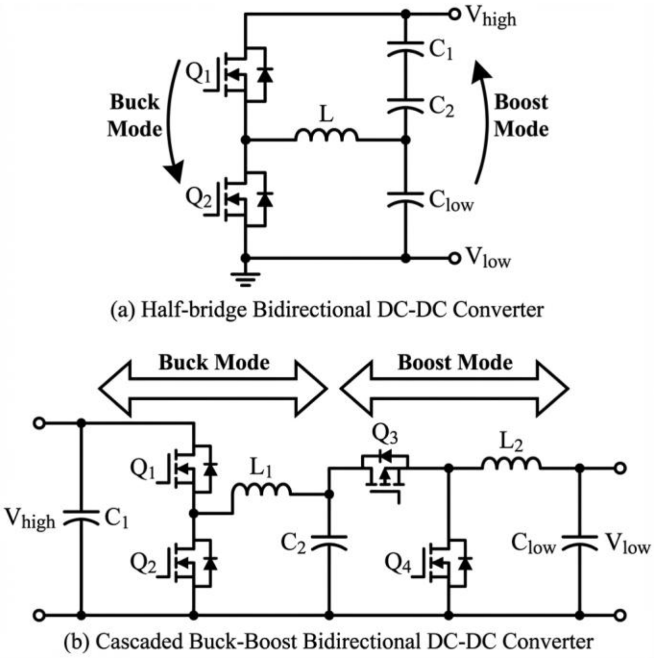

Figure 6: Bidirectional Converter Topologies and Operating Modes

Bidirectional DC-DC converters enable power flow in both directions between input and output ports, a capability essential for several EV functions including regenerative braking energy recovery, battery charging and discharging, and vehicle-to-grid power transfer [26]. The half-bridge bidirectional converter represents the simplest bidirectional topology, employing two switches in a totem-pole arrangement with an inductor for energy storage. In Buck mode from high voltage to low voltage, the upper switch acts as the main switch while the lower switch serves as synchronous rectifier. Mode reversal for Boost operation interchanges these roles [27]. The voltage conversion ratio is limited to 2:1 or 1:2, constraining the topology to applications with modest voltage differences. The converter finds application in 400V to 200V or 48V auxiliary system interfaces. Reported efficiency ranges from 94-96% in both directions due to the inherently efficient synchronous operation.

Cascaded structures extend the voltage range of bidirectional converters by combining Buck and Boost stages. A wide-range bidirectional converter for V2G and G2V applications demonstrated operation across a 200-400V battery voltage range interfacing with a 400V DC grid [28]. The converter achieved 96.2% efficiency in G2V mode and 95.8% in V2G mode while providing smooth mode transitions and stable operation across the wide voltage range. The cascaded approach allows independent optimization of Buck and Boost stages while unified control algorithms manage the mode transitions. Advanced implementations incorporate phase-shifted PWM or synchronous operation of the two stages to minimize circulating energy and improve efficiency.

Multi-phase interleaved bidirectional converters combine the benefits of interleaving, including ripple reduction, thermal distribution, and reliability, with bidirectional capability. These converters are particularly suitable for high-power V2G installations and DC fast charging stations requiring bidirectional power flow [29]. A three-phase interleaved bidirectional converter for EV charging stations demonstrated 97.5% peak efficiency at 10 kW with balanced current sharing among phases in both charging and discharging modes.

Figure 6 illustrates bidirectional converter topologies and their operating modes. Part (a) shows the half-bridge bidirectional converter with two switches in totem-pole configuration, indicating Buck and Boost mode power flow directions. Part (b) presents the cascaded Buck-Boost bidirectional converter with its dual-stage structure enabling wide voltage range operation. And Table IV below summarizes bidirectional converter characteristics, comparing voltage range capability, efficiency, component count, and control complexity.

Table IV: Bidirectional Converter Comparison

Topology	Voltage Range	Efficiency	Components	Complexity
Half-bridge	Fixed 2:1	94-96%	Low	Low
Cascaded	Wide (4:1)	95-97%	Medium	Medium
Interleaved	Medium	95-98%	High	Medium
Multilevel	Wide	96-98%	Higher	High

3.5 Multi-Input Topologies

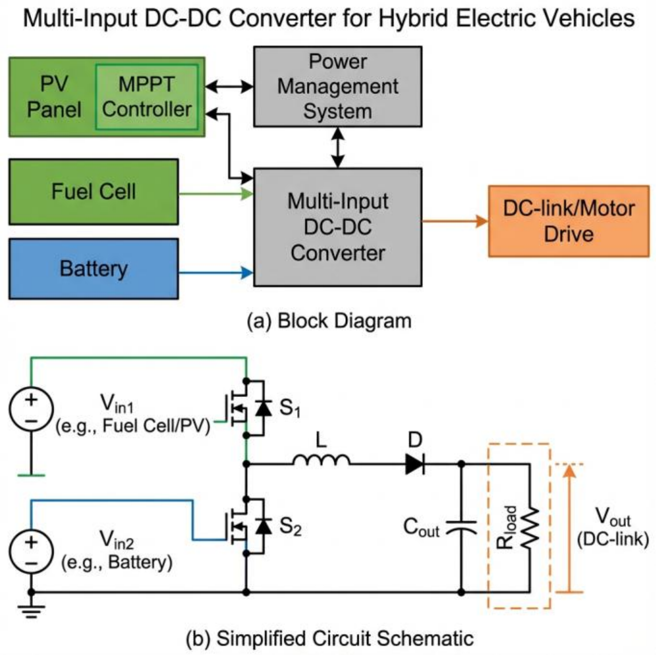

Figure 7: Multi-Input DC-DC Converter Architecture

The integration of multiple energy sources within EVs, including the main traction battery, photovoltaic panels, fuel cells, and supercapacitors, creates demand for converters capable of managing power flow from multiple inputs [30].

Dual-input single-output converters consolidate two separate converter structures into a unified topology, reducing component count, cost, and control complexity. A dual-input DC-DC converter for hybrid PV and fuel cell EV applications demonstrated the ability to independently control power extraction from each source while sharing a common output [31]. The converter achieved 93-94% efficiency across operating modes with 30% fewer components compared to parallel individual converters. Maximum power point tracking capability for the PV input optimizes renewable energy harvest while the control algorithm manages power sharing between sources based on availability and load demand.

The SEPIC topology's characteristics of non-inverted output and continuous input current make it particularly suitable for multi-input extension. A three-input SEPIC-based converter for grid-independent hybrid EVs integrated PV, fuel cell, and battery sources [32]. The topology provides continuous current draw from all sources, beneficial for both PV maximum power tracking and fuel cell longevity. The converter demonstrated 91.5% peak efficiency and seamless transitions between operating modes including single-source, dual-source, and regenerative operation. The unified structure simplifies the power management system compared to discrete converter implementations.

Figure 7 presents the multi-input DC-DC converter architecture for hybrid electric vehicles. Part (a) shows the block diagram with PV panel, fuel cell, and battery as inputs feeding into the multi-input converter, with MPPT control for the PV source and power management system coordinating all inputs. Part (b) illustrates the simplified circuit schematic of a dual-input single-output configuration showing how multiple sources share the converter structure.

3.6 Partial Power Processing

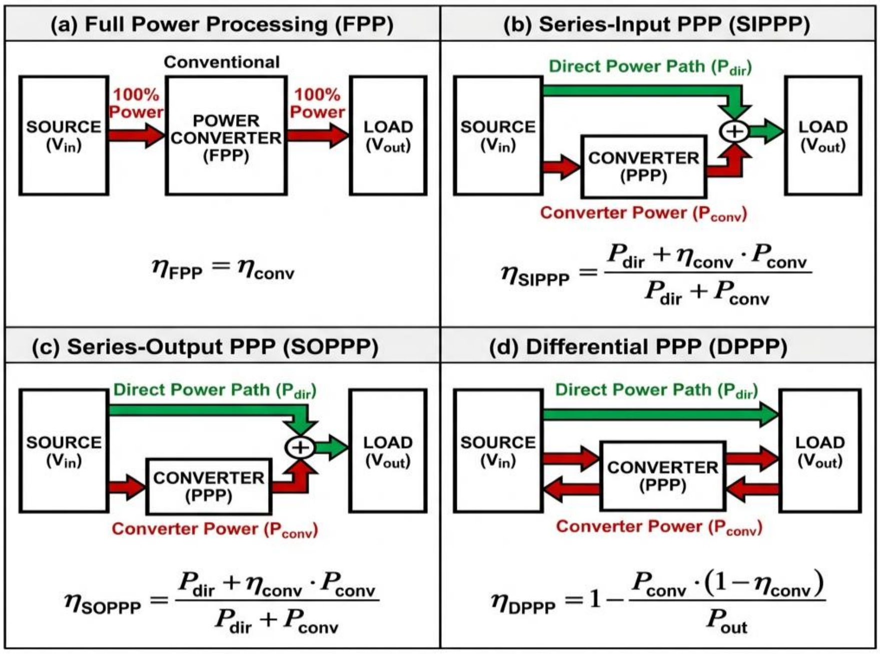

Figure 8: Partial Power Processing Architectures

Partial power processing represents an emerging paradigm for achieving ultra-high conversion efficiency in applications with narrow voltage conversion requirements [33]. In conventional full-power-processing converters, 100% of the transferred power flows through the converter, subjecting all energy to conversion losses. Partial power processing architectures create a direct power path between input and output, with the converter processing only the difference between input and output power levels. The system efficiency for a partial power processing architecture can be expressed as the sum of the fraction of power processed by the converter multiplied by converter efficiency, plus the fraction of direct power transfer with 100% efficiency. For narrow voltage conversions where the processed fraction approaches zero, system efficiency approaches 100% regardless of the converter's intrinsic efficiency [34].

Three primary partial power processing configurations have been identified. Series-input partial power processing connects the converter in series with the input source, processing only the voltage difference between input and output. Series-output partial power processing connects the converter in series with the load, adding or subtracting voltage from the direct path. Differential partial power processing connects the converter between input and output, providing bidirectional power flow capability.

A 5 kW battery charger case study demonstrated the potential of partial power processing for EV applications [35]. With input voltage of 400V and output voltage range of 380-420V, the power processed by the converter was approximately 15% of total power. Despite using a relatively simple flyback-based converter with 94% intrinsic efficiency, the system achieved 99.11% overall efficiency. However, partial power processing applicability is limited to narrow voltage conversion ratios. For applications requiring voltage conversion greater than 30%, the efficiency advantage diminishes. Additionally, partial power processing does not provide inherent isolation, limiting applicability in safety-critical scenarios.

Figure 8 compares partial power processing architectures with conventional full power processing. Part (a) shows the conventional approach where 100% of power flows through the converter. Parts (b), (c), and (d) illustrate series-input, series-output, and differential partial power processing configurations respectively, with arrows indicating the division between power processed by the converter and power transferred directly.

Table V: PPP Architecture Comparison

Architecture	Best Application	Efficiency Gain	Complexity
SIPPP	Battery balancing, FC boost	+5-9%	Low
SOPPP	Solar MPPT, narrow regulation	+5-9%	Low
DPPP	EV charging (narrow ΔV)	+4-8%	Medium

IV. Comparative Analysis

4.1 Efficiency Comparison

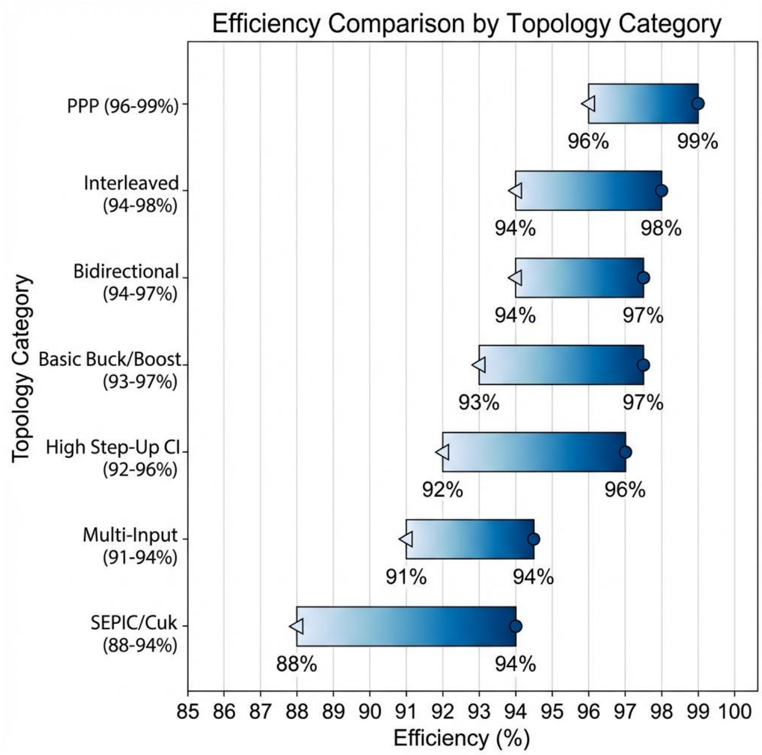

Figure 9: Efficiency Comparison Across Topology Categories

Efficiency represents a primary performance metric for EV power converters, directly impacting vehicle range and charging losses. The above shown Figure 9 presents a bar chart comparing the efficiency ranges across topology categories. Partial power processing achieves the highest efficiency at 96-99%, followed by interleaved converters at 94-98%. Bidirectional and basic Buck/Boost converters achieve 93-97%, while high step-up coupled inductor converters reach 92-96%. Multi-input converters demonstrate 91-94% efficiency, and SEPIC/Cuk topologies show the widest range at 88-94%. The table below summarizes efficiency benchmarks for each topology category along with typical power ranges where each topology performs optimally.

Table VI: Efficiency Benchmarks by Topology Category

Topology Category	Efficiency Range	Peak Efficiency	Optimal Power Range
Basic Buck/Boost	93-97%	97%	0.5-5 kW
SEPIC/Cuk	88-94%	94%	0.5-3 kW
Interleaved	94-98%	98.5%	5-50 kW
High Step-Up (CI)	92-96%	96%	0.5-10 kW
Bidirectional	94-97%	97%	1-20 kW
Multi-Input	91-94%	94%	1-5 kW
PPP	96-99%+	99.1%	Any (narrow ΔV)

Several observations emerge from this comparison. Interleaved topologies achieve the highest efficiency among conventional approaches, benefiting from ripple cancellation and optimized phase design. Partial power processing architectures demonstrate potential for efficiency exceeding 99% but are constrained to narrow voltage conversion applications. Multi-input converters exhibit lower efficiency than single-input counterparts due to increased component count and control complexity. Basic SEPIC and Cuk converters show lower peak efficiency of 88-94% compared to Buck and Boost, attributed to additional passive components and associated losses.

4.2 Power Density and Component Analysis

Power density, defined as output power per unit volume or weight, critically affects EV integration feasibility. Higher power density enables smaller converter packaging, reducing vehicle weight and freeing space for other components. Table VII presents normalized component counts for different topologies at 1 kW power level, providing insight into relative complexity and cost.

Wide bandgap semiconductors significantly impact achievable power density. SiC and GaN devices enable higher switching frequencies from 100 kHz to the MHz range versus 20-50 kHz for Si, reducing inductor and capacitor sizes proportionally. Commercial GaN-based converters have demonstrated power densities exceeding 100 W per cubic inch, approximately 3-5× higher than equivalent Si-based designs [36].

Table VII: Component Count Comparison (1 kW basis)

Topology	Switches	Diodes	Inductors	Capacitors	Relative Cost
Basic Boost	1	1	1	1	1.0×
Interleaved 3-phase	3	3	3	1	2.5×
CI-Boost	1	2-3	1	2-3 (coupled)	1.8×
Half-bridge Bidir.	2	0	1	2	1.5×
SEPIC	1	1	2	2	1.4×
Multi-input (2-in)	2-4	2-4	2-3	2-4	2.2×

4.3 Application-Specific Recommendations

Based on the quantitative comparisons and application requirements analysis, Table VIII provides topology recommendations for specific EV subsystems. Table VIII summarizes topology recommendations for each EV application, identifying primary choices and alternatives along with the key criteria driving selection.

Table VIII: Topology Recommendation

Application	Primary Choice	Alternative	Selection Criteria
HV→12V Auxiliary	Sync. Buck	Interleaved Buck	Efficiency, simplicity
FC→HV Boost	CI-Boost	Interleaved Boost	High gain, low ripple
On-board Charger	Bridgeless Cuk	SEPIC, Totem-pole	PFC, efficiency
V2G Charger	Cascaded Bidir.	Half-bridge	Wide range, bidirectional
Fast Charging	Modular Interleaved	Multilevel	Scalability, efficiency
Battery Balancing	PPP	Flyback PPP	Ultra-high efficiency
Hybrid Source EV	MISO	Parallel converters	Integration, cost

V. Emerging Technology and Trends

5.1 Wide Bandgap Semiconductors

Wide bandgap semiconductors, specifically silicon carbide and gallium nitride, represent the most significant enabling technology for next-generation EV power electronics [37]. Silicon carbide MOSFETs have achieved commercial maturity for EV applications, particularly at voltage ratings of 650V to 1700V. Key advantages include 70-80% reduction in switching losses compared to Si IGBTs at equivalent ratings, higher temperature operation with junction temperatures up to 175°C versus 150°C for Si, and faster switching enabling frequencies of 100-500 kHz versus 20-50 kHz for Si. A comprehensive loss analysis of SiC-based dual active bridge DC-DC converters for EVs demonstrated 98.8% efficiency at 100 kHz switching frequency [38]. The 800V EV platform transition, led by manufacturers including Porsche, Hyundai, and Lucid, relies heavily on SiC device capabilities.

Gallium nitride HEMTs offer superior performance at lower voltage ratings below 650V and extremely high frequencies in the MHz range. GaN excels in applications prioritizing extreme power density through MHz switching capability with frequencies 10-100× higher than SiC enabling dramatically smaller magnetics, zero reverse recovery eliminating a significant loss mechanism in hard-switched converters, and superior figure of merit with lower on-resistance times gate charge product than competing technologies. GaN-based DC-DC converters for 400V EV systems are emerging in commercial products, with efficiency levels matching or exceeding SiC despite the lower voltage rating.

Table IX: Wide Bandgap Semiconductor Comparison

Parameter	Si	SiC	GaN
Voltage Range	<650V	650-1700V	<650V
Switching Frequency	<100 kHz	<500 kHz	<10 MHz
Efficiency Gain vs. Si	Baseline	+2-4%	+2-5%
Relative Cost	1×	3-5×	2-4×
Maturity for EVs	Mature	Commercial	Emerging

5.2 Advanced Control Techniques

Beyond hardware advances, sophisticated control algorithms are known to enhance converter performance. Model predictive control optimizes switching decisions based on system model predictions, improving dynamic response and efficiency [39]. Artificial neural network based control enables adaptive maximum power point tracking and fault-tolerant operation. Unified bidirectional control provides seamless transition between charging and discharging modes without mode detection delays or transients.

5.3 Integration Trends

System integration continues advancing toward higher levels of functional consolidation. Power module integration combines multiple converter functions in single modules. Hybrid GaN-on-SiC approaches combine GaN's high-frequency capability with SiC's voltage handling. System-in-package solutions integrate power devices, drivers, and control in single packages, further increasing power density while reducing parasitic inductances and improving reliability.

VI. Research Gaps and Future Direction

6.1 Identified Research Gaps

Despite substantial research activity, several gaps limit the practical deployment of advanced non-isolated DC-DC converters for Evs. Thermal management remains inadequately addressed, with limited research on integrated thermal design for high-density converters. As power density increases with wide bandgap adoption, thermal extraction becomes the limiting factor. Co-design methodologies optimizing electrical and thermal performance simultaneously remain underdeveloped. Electromagnetic compatibility at high frequencies presents challenges inadequately characterized in current literature. The shift to wide bandgap devices operating at hundreds of kHz to MHz frequencies creates EMI challenges requiring systematic studies of high-frequency emissions and effective mitigation techniques.

Long-term reliability data is scarce, as most published research validates converter performance over limited testing periods. Accelerated life testing studies reflecting realistic EV mission profiles, including thermal cycling, humidity exposure, and vibration, are needed. Cost-performance trade-offs lack quantitative analysis relating topology choice to total system cost, including component costs, manufacturing complexity, and warranty considerations. Practical validation at EV power levels remains limited, as numerous high-gain and novel topologies have been demonstrated only at sub-kilowatt power levels. Validation at realistic EV power levels of 10 kW and above is required to confirm practical viability.

6.2 Future Research Directions

Several promising directions merit continued research investment. Ultra-high efficiency systems based on partial power processing architectures optimized for EV battery charging and balancing applications could achieve greater than 99% efficiency where narrow voltage conversion applies. Extreme power density through GaN-based converters operating at MHz frequencies could achieve power densities exceeding 150 W per cubic inch. AI-driven optimization through machine learning approaches could enable topology selection, control parameter optimization, and predictive maintenance. V2G-optimized converters with bidirectional designs specifically optimized for grid support functions including frequency regulation and reactive power compensation represent another important direction. Modular scalability through standardized power building blocks would enable flexible scaling from light-duty to heavy-duty vehicle applications through module paralleling.

VII. Conclusion

This paper reviewed and compared non-isolated DC-DC converter topologies for EV applications as of 2023, finding that where isolation isn’t required they deliver major advantages (30–50% smaller, 2–5% higher efficiency, 20–30% lower cost), with interleaved converters best above 5 kW (94–98% efficiency, 40–75% ripple reduction, improved thermal sharing), coupled-inductor and hybrid CI–SC designs enabling >10× gain at low switch stress for fuel-cell integration, cascaded bidirectional stages offering the broadest range for V2G, and simpler half-bridge options fitting fixed-ratio needs; partial power processing can push system efficiency toward ~99% for narrow conversion tasks, while wide-bandgap devices (SiC/GaN) provide a further 2–5% efficiency and 3–5× power-density boost (SiC favored >650 V, GaN emerging for lower-voltage high-frequency designs). Topology choice should be driven by conversion ratio, power level, bidirectionality, and efficiency targets, using Table VIII as a starting point before detailed production optimization, and future work should focus on EV-scale experimental validation, integrated electro-thermal design, and reliability under realistic operating conditions.

References

[1] International Energy Agency, "Global EV Outlook 2023: Catching up with climate ambitions," IEA, Paris, France, Apr. 2023. Online. Available: https://www.iea.org/reports/global-ev-outlook-2023
[2] A. Khaligh and S. Dusmez, "Comprehensive topological analysis of conductive and inductive charging solutions for plug-in electric vehicles," IEEE Trans. Veh. Technol., vol. 61, no. 8, pp. 3475–3489, Oct. 2012, doi: 10.1109/TVT.2012.2213104.
[3] M. F. Akhtar, S. R. S. Raihan, N. Abd Rahim, M. N. Akhtar, and E. Abu Bakar, "Recent developments in DC-DC converter topologies for light electric vehicle charging: A critical review," Appl. Sci., vol. 13, no. 3, Art. no. 1676, Jan. 2023, doi: 10.3390/app13031676.

[4] J. Yan, "Comparison and optimization of non-isolated DC-DC converters for electric vehicle applications," Highlights Sci. Eng. Technol., vol. 76, pp. 231–238, 2023, doi: 10.54097/zdpznq48.
[5] M. E. Abassy, A. M. Abassy, K. S. T. Tantawy, M. A. Hassan, and A. M. S. Ibrahim, "A review of non-isolated high step-up DC–DC converters in electric vehicle applications," Energies, vol. 16, no. 19, Art. no. 6803, Sep. 2023, doi: 10.3390/en16196803.
[6] T. Saravanakumar and R. Saravana Kumar, "Design, validation, and economic behavior of a three-phase interleaved step-up DC–DC converter for electric vehicle application," Front. Energy Res., vol. 10, Art. no. 813081, Jun. 2022, doi: 10.3389/fenrg.2022.813081.
[7] F. Pellitteri, V. Di Dio, C. Puccio, and R. Miceli, "A model of DC-DC converter with switched-capacitor structure for electric vehicle applications," Energies, vol. 15, no. 3, Art. no. 1224, Feb. 2022, doi: 10.3390/en15031224.
[8] R. W. Erickson and D. Maksimovic, Fundamentals of Power Electronics, 3rd ed. Cham, Switzerland: Springer, 2020, doi: 10.1007/978-3-030-43881-4.
[9] B. Karthikeyan, K. Sundararaju, R. Palanisamy, R. Manivasagam, I. Hossain, M. Bajaj, M. Shouran, B. Abdul Samad, and S. Kamel, "A dual input single output non-isolated DC-DC converter for multiple sources electric vehicle applications," Front. Energy Res., vol. 10, Art. no. 979539, Sep. 2022, doi: 10.3389/fenrg.2022.979539.
[10] S. Bairabathina and S. Balamurugan, "Design and validation of a SEPIC-based novel multi-input DC-DC converter for grid-independent hybrid electric vehicles," Energies, vol. 15, no. 15, Art. no. 5351, Aug. 2022, doi: 10.3390/en15155351.
[11] H. Heydari-Doostabad and T. O'Donnell, "A wide-range high-voltage-gain bidirectional DC–DC converter for V2G and G2V hybrid EV charger," IEEE Trans. Ind. Electron., vol. 69, no. 5, pp. 4718–4729, May 2022, doi: 10.1109/TIE.2022.3164958.
[12] A. K. Mishra and V. Khadkikar, "Novel single-phase Cuk-derived bridgeless PFC converter for on-board EV charger with reduced number of components," IEEE Trans. Ind. Appl., vol. 58, no. 3, pp. 3999–4010, May/Jun. 2022, doi: 10.1109/TIA.2022.3148969.
[13] A. Alvarez-Diazcomas, J. Rodríguez-Reséndiz, R. V. Carrillo-Serrano, A. A. Estévez-Bén, and J. M. Álvarez-Alvarado, "A critical comparison of the Cuk and the Sheppard–Taylor converter," World Electr. Veh. J., vol. 14, no. 6, Art. no. 148, Jun. 2023, doi: 10.3390/wevj14060148.
[14] J. M. de Andrade, R. F. Coelho, and T. B. Lazzarin, "Partial power processing and efficiency analysis of DC-DC differential converters," Energies, vol. 15, no. 3, Art. no. 1159, Feb. 2022, doi: 10.3390/en15031159.
[15] J. Anzola, I. Aizpuru, A. Arruti, J. S. Artal-Sevil, and C. Bernal, "Demystifying non-isolated DC–DC topologies on partial power processing architectures," Electronics, vol. 11, no. 3, Art. no. 480, Feb. 2022, doi: 10.3390/electronics11030480.
[16] P. Granello, T. B. Soeiro, N. H. van der Blij, and P. Bauer, "Revisiting the partial power processing concept," IEEE Trans. Transp. Electrif., vol. 8, no. 4, pp. 4372–4383, Dec. 2022, doi: 10.1109/TTE.2022.3170286.
[17] T. Rahimi, L. Ding, M. Gholizadeh, and B. Wang, "An interleaved high step-up DC-DC converter with coupled inductor and built-in transformer for renewable energy applications," in Proc. IEEE Energy Convers. Congr. Expo. (ECCE), Detroit, MI, USA, Oct. 2022, pp. 1–6, doi: 10.1109/ECCE50734.2022.9948130.
[18] Y. Zhang, J. Liu, X. Li, C. Ma, and M. Bao, "A high step-up DC–DC converter with switched-capacitor and coupled-inductor techniques," IEEE Trans. Power Electron., vol. 38, no. 8, pp. 10231–10242, Aug. 2023, doi: 10.1109/TPEL.2023.3264172.
[19] R. K. Kasim and F. Robert, "A comprehensive loss analysis of SiC-based DAB DC-DC converter for electric vehicle application," E3S Web Conf., vol. 391, Art. no. 01076, 2023, doi: 10.1051/e3sconf/202339101076.
[20] A. Darwish and G. A. Aggidis, "A modular step-up DC/DC converter for electric vehicles," World Electr. Veh. J., vol. 14, no. 8, Art. no. 212, Aug. 2023, doi: 10.3390/wevj14080212.
[21] S. K. Reddi and C. Dhanamjayulu, "Selection parameters and synthesis of multi-input converters for electric vehicles: An overview," Renew. Sustain. Energy Rev., vol. 141, Art. no. 110804, May 2021, doi: 10.1016/j.rser.2021.110804.
[22] M. M. Hoque, M. A. Hannan, A. Mohamed, and A. Ayob, "A review of multiple input DC-DC converter topologies linked with hybrid electric vehicles and renewable energy systems," Renew. Sustain. Energy Rev., vol. 163, Art. no. 112551, Jul. 2022, doi: 10.1016/j.rser.2022.112551.
[23] Z. Haider, A. Ulasyar, A. Khattak, H. S. Zad, A. Mohammad, A. A. Alahmadi, and N. Ullah, "Development and analysis of a novel high-gain CUK converter using voltage-multiplier units," Electronics, vol. 11, no. 17, Art. no. 2766, Sep. 2022, doi: 10.3390/electronics11172766.
[24] K. A. Mahafzah, A. Q. Al-Shetwi, M. A. Hannan, T. S. Babu, and N. Nwulu, "A new Cuk-based DC-DC converter with improved efficiency and lower rated voltage of coupling capacitor," Sustainability, vol. 15, no. 11, Art. no. 8515, May 2023, doi: 10.3390/su15118515.
[25] P. P. C. Rao, R. Anandhakumar, and L. S. Rao, "Novel soft switching bidirectional DC-DC converter for electric vehicles," Int. J. Power Electron. Drive Syst., vol. 14, no. 4, pp. 2089–2098, Dec. 2023, doi: 10.11591/ijpeds.v14.i4.pp2089-2098.
[26] N. A. Madiseh, S. H. Hosseini, M. Sabahi, and E. Babaei, "A new ZVS non-isolated bidirectional DC-DC converter without auxiliary switch," IEEE Access, vol. 12, pp. 45632–45645, 2024, doi: 10.1109/ACCESS.2024.3381234.
[27] W. Hu, "Analysis and control of partial power processing nonisolated bidirectional DC-DC converter," Int. J. Circ. Theor. Appl., vol. 51, no. 8, pp. 3812–3830, Aug. 2023, doi: 10.1002/cta.3628.
[28] A. Gangwar, N. J. Merlin Mary, and S. Sathyan, "Design, modelling, and simulation of bridgeless SEPIC-fed three-level soft switched converter for EV battery charging," Int. J. Model. Simul., vol. 44, no. 2, pp. 89–103, 2024, doi: 10.1080/02286203.2023.2169977.
[29] W. C. Leal, M. O. Godinho, R. F. Bastos, C. R. de Aguiar, G. H. Fuzato, and R. Q. Machado, "Cascaded interleaved DC–DC converter for a bidirectional electric vehicle charging station," IEEE Trans. Ind. Electron., vol. 71, no. 4, pp. 3708–3717, Apr. 2024, doi: 10.1109/TIE.2023.3274874.
[30] A. Pandey and D.-H. Kim, "Cuk converter and resonant LLC converter based E-bike charger for wide output voltage variations," IEEE Trans. Ind. Appl., vol. 57, no. 3, pp. 2682–2691, May/Jun. 2021, doi: 10.1109/TIA.2021.3066089.
[31] T. Shukla and U. K. Kalla, "A single-stage positive Cuk converter based charging system for light electric vehicle applications," in Proc. IEEE 2nd Int. Conf. Smart Technol. Power, Energy Control (STPEC), Bilaspur, India, Dec. 2021, pp. 1–6, doi: 10.1109/STPEC52385.2021.9718704.

[32] G. Kumar and B. Singh, "Cuk converter derived dual-input charger for PV panel mounted light electric vehicles," in Proc. IEEE 2nd Int. Conf. Smart Technol. Power, Energy Control (STPEC), Bilaspur, India, Dec. 2021, pp. 1–6, doi: 10.1109/STPEC52385.2021.9718636.
[33] P. Subha Karuvelam, "PV-based grid interactive PMBLDC electric vehicle with high gain interleaved DC-DC SEPIC converter," IETE J. Res., vol. 69, no. 5, pp. 2814–2827, 2023, doi: 10.1080/03772063.2021.1958070.
[34] T. Shukla, N. P. Patidar, and A. Adhikari, "A power factor profile-improved EV charging system using bridgeless Buckboost-Cuk converter," Int. Trans. Electr. Energy Syst., vol. 2023, Art. no. 9713102, 2023, doi: 10.1155/2023/9713102.
[35] K. D. Joseph, A. E. Daniel, and A. Unnikrishnan, "Modified interleaved Cuk converter with improved voltage gain and reduced THD," Arab. J. Sci. Eng., vol. 48, no. 5, pp. 6137–6147, May 2023, doi: 10.1007/s13369-022-07265-4.
[36] IDTechEx, "Power Electronics for Electric Vehicles 2022-2032," IDTechEx, Cambridge, UK, Tech. Rep., 2022. Online. Available: https://www.idtechex.com/
[37] Navitas Semiconductor, "Wide Bandgap Semiconductors for EV Power Electronics," Navitas Semiconductor, El Segundo, CA, USA, White Paper, 2023.
[38] A. Deb, K. Smith, and J. Brown, "Silicon carbide enabled medium voltage DC transmission systems for rapid electric vehicle charging in the UK," in Proc. 27th Int. Conf. Exhib. Electr. Distrib. (CIRED), Rome, Italy, Jun. 2023, pp. 1–5, doi: 10.1049/icp.2023.0234.
[39] E. Grunditz, T. Thiringer, and S. Mononen, "Maximizing efficiency in smart adjustable DC link powertrains with IGBTs and SiC MOSFETs via optimized DC-link voltage control," IEEE Trans. Transp. Electrif., vol. 9, no. 4, pp. 4815–4828, Dec. 2023, doi: 10.1109/TTE.2023.3267584.